

# Pursuit and Evasion with Uncertain Bearing Measurements

Josh Vander Hook and Volkan Isler\*

## Abstract

We study pursuit-evasion games in which a deterministic pursuer tries to capture an evader by moving onto the evader’s position. We investigate how sensing capability of the pursuer affects the game outcome. In particular, we consider a pursuer which can sense only the bearing to an evader. Furthermore, there is noise in the measurements such that an adversary may adjust each bearing measured by an angle up to  $\alpha$  away from the true value.

We consider two classical pursuit evasion games under this bearing uncertainty model. The first game is played on the open plane. The pursuer tries to maintain the distance to an evader with equal speed. If the pursuer has full knowledge of the evader’s location the pursuer can maintain the separation between the players by moving toward the evader. However, when an adversarial sensing model is introduced, we show that for any pursuer strategy, the evader can increase the distance to the pursuer indefinitely. The rate at which the distance increases is linear in time.

In the second game, both players are inside a bounded circular area. This version is known as the Lion-and-Man game, and has been well studied when no sensing limitations are imposed. In particular, the pursuer (Lion) is known to have an  $O(r \log r)$  strategy to capture the evader, where  $r$  is the radius of the circle. In contrast, when sensing uncertainty is introduced, we show that for any  $\alpha > 0$ , there exist circular environments in which the man can evade capture indefinitely.

## 1 Introduction

In a typical pursuit-evasion game, a pursuer tries to capture an evader who in turn tries to avoid capture. Earlier pursuit-evasion games were studied as recreational mathematics problems. For example, in the lion-and-man game presented in [1] a lion tries to capture a man in a circular arena. In recent years, pursuit-evasion games have received significant attention due to their applications in robotics and related fields [2].

In the last couple of years, our group has been working on building a system of autonomous boats for tracking

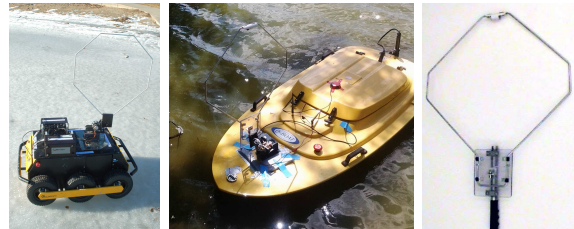


Figure 1: The robots designed for tracking fish during the winter (left) and summer (middle). The direction-sensitive antenna mounted on the robots (right). The bearing to the target can be estimated by rotating the antenna every  $\alpha$  degrees. The bearing corresponding to the maximum signal strength is taken as the true bearing. Thus, the uncertainty is at most  $\alpha$ .

radio-tagged invasive fish [3]. In our system, each boat can rotate its directional antenna to measure the bearing of a fish. See Figure 1. The goal is to track the movement of the fish using these measurements. Modeling such tracking problems as pursuit-evasion games is advantageous because we do not have good models for how the fish move. By modeling the targets as adversaries that are trying to escape and designing corresponding pursuit strategies, we can obtain tracking strategies which work regardless of the motion of the fish. Furthermore, by considering adversarial sensing, tracking strategies are made robust against sensor biases or incorrect sensing models.

For such pursuit strategies to be practically applicable, they must work under realistic sensing models. Unfortunately, traditional formulations assume idealized measurements. For example, consider the lion-and-man game in which a lion tries to capture a man in a circular arena [1]. The players have equal maximum velocities. The lion can obtain the exact location of the man at all times. In contrast, in most robotics settings the location of the target is not available. In our fish tracking application, the pursuer can measure only the bearing rather than the exact location. Moreover, the measurements are uncertain: if we rotate the antenna  $2\alpha$  degrees between consecutive measurements and obtain the angle with the highest signal value, our estimate of the bearing can be off by  $\alpha$  degrees.

In this work, we study pursuit-evasion games in which the pursuer can obtain only uncertain bearing measure-

\*The authors are with the Department of Computer Science and Engineering, University of Minnesota, Minneapolis, MN, USA. {jvander, isler}@cs.umn.edu

ments. Bearing sensors, in particular cameras and microphone arrays, are commonly used in robotics and sensor network applications. We provide two results.

First, we look into the simple setting of chasing the evader in the open plane. When the players have the same speed, the best the pursuer can do is to maintain the initial distance between the players by moving toward the evader along the line connecting them. The evader can ensure that the separation is maintained by moving away from the pursuer in the same direction. The pursuer can execute this strategy even if he obtains only bearing measurements (rather than the exact location of the evader). In Section 2, we show that, if there is any uncertainty in bearing measurements, the evader can increase the distance between the players. Specifically, we show that for any pursuer strategy, there exists an evasion strategy which guarantees that the distance between the players increases indefinitely.

Second, we study the lion-and-man game in a circular arena. Intuitively, it is easy to see that the pursuer can get closer and closer to the evader by moving toward it. This is because the evader has to move away from the pursuer to maintain separation which is not possible indefinitely in a bounded arena. Every time the evader turns, the distance between the players decreases. Note that this greedy strategy can be executed even when the pursuer can obtain only bearing measurements<sup>1</sup>. In Section 3, we show that the outcome favors the evader if there is uncertainty in the measurements. We show that, for any uncertainty value  $\alpha$ , there are circular environments in which the evader can escape by presenting an evasion strategy.

## 1.1 Related Work

There are numerous pursuit-evasion games. A survey of robotics-related pursuit evasion games can be found in [2]. However, very few game models consider sensing uncertainty. A notable exception is the result by Rote who studied the problem of chasing the target in the open plane [5]. In his model, the evader can hide its true location and present any location within distance  $d$  from his true location as the measurement. It was shown that the evader can increase his distance from the pursuer at a rate of  $\Theta(\sqrt[3]{t})$ , where  $t$  is the time spent playing. In case of bearing measurements, we show that the evader can do much better and ensure that the increase in the distance is linear in  $t$ . Independent from this work, Klein showed a linear rate for a distance-dependent position error [6] with and without obstacles in the open plane.

In the next section, we start by studying the game on the open plane, followed by the Lion and Man version in

<sup>1</sup>This is not the most efficient pursuit strategy. Alonso et al. present a near optimal strategy for capture [4]. Their strategy however requires measuring the exact location of the man.

Section 3. For convenience, in the appendix we present notation and explanations of variables used throughout the paper.

## 2 Open Plane Pursuit

In this section we describe the evader’s strategy to win the open-plane pursuit. We first cover the game model. Let the position of the evader and pursuer at the beginning of turn  $t$  be  $e(t)$  and  $p(t)$  respectively. Each turn proceeds as follows. First, the pursuer measures the angle  $b(t) = b^*(t) + \alpha(t)$ , where  $b^*(t)$  is the true bearing to the evader and  $\alpha(t)$  is the offset applied by the evader, subject to  $|\alpha(t)| \leq \alpha$ . Next, the pursuer chooses his next location  $p(t+1)$  subject to  $\|p(t+1) - p(t)\| \leq 1$ . The strategy by which the pursuer chooses his next location is given by the deterministic policy  $\pi : (P, B) \rightarrow p(t+1)$ , where  $P = \{p(1), p(2), \dots, p(t)\}$  is the previous pursuer positions, and  $B = \{b(1), b(2), \dots, b(t)\}$  is all the measurements received by the pursuer up to time  $t$ . Next, the evader moves to  $e(t+1)$  where  $\|e(t+1) - e(t)\| \leq 1$ .

It is worth noting that we allow the evader to have full knowledge of the policy chosen by the pursuer. Since the pursuer is deterministic, this gives the evader the power to predict the pursuer’s actions as a function of his measurement history. We show that there is no pursuer policy which can account for all evader strategies even though the pursuer can obtain bearing measurements along the way.

### 2.1 Evader Strategy

We will show that *for any* deterministic pursuer policy  $\pi$ , the evader can specify a trajectory and measurement sequence to increase the distance between the pursuer and evader. Let  $\pi_p$  be the pursuer’s specified strategy. The evader strategy proceeds in rounds, each consisting of  $N$  turns. The evader will first *simulate* a possible measurement sequence,  $B$ , and observe the output of the policy  $\pi_p(P, B)$  (i.e., the pursuer’s trajectory). Based on the pursuer’s trajectory, the evader will choose a trajectory to follow, but will use the same measurement sequence,  $B$ , used in the simulation step. Since the pursuer’s response is a function of only the *measurements*, the evader can follow a different trajectory without altering the pursuer response, as long as the measurements remain the same.

As shown in Figure 3, let the line  $\overline{p(0)e(0)}$  be the  $x$  axis of a coordinate frame which remains fixed for the current round. Let  $d(0)$  be the separation between  $p(0)$  and  $e(0)$  at the beginning of the round. There are two parameters to the simulation, a constant  $T_\alpha$  and  $\rho$ . Here,  $N = T_\alpha \cdot d(0)$  is the length of the round (in turns) and is specified by the evader, and  $\rho$  is an acute angle (offset from  $\overline{p(0)e(0)}$ ) which is less than  $\alpha$ .  $T_\alpha$  is given as follows (and is derived in Theorem 4). The

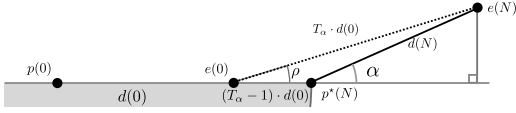


Figure 2: The pursuer starts location  $p(0)$  and the evader at  $e(0)$  separated by distance  $d(0)$ . After  $N$  steps, the pursuer is in a closed disc  $C$  of radius  $N$  centered at  $p(0)$ . The key component of the evader strategy is to generate two motions which produce the same set of bearing measurements. Since the pursuer's strategy is deterministic (as a function of the bearing measurement), the evader knows which half of  $C$  the pursuer ends in (above or below the line  $\overline{p(0)e(0)}$ ). If the pursuer is anywhere in the lower half of  $C$ , (shaded portion), the evader will be at location  $e(N)$ . The closest position the pursuer can take is at  $p^*(N)$ , and the ending distance between the players is given by  $d(N)$ . The case if the pursuer is above or on the line is symmetric.

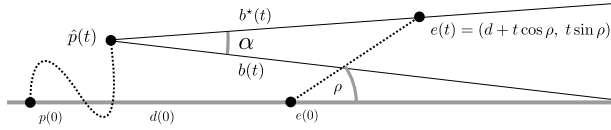


Figure 3: The evader's simulation, which is used to find the final pursuer's location after  $N$  steps, given measurement sequence  $B$ . The evader path is shown along with one possible pursuer path. The true bearing ( $b^*(t)$ ) and offset bearing ( $b(t)$ ) are solid lines.

value of the constant  $T_\alpha$  was chosen to maximize the final distance at the end of the round (as a function of  $\alpha$ ).

$$T_\alpha = \left(1 - \sqrt{\frac{1}{2 + 2 \cos \alpha}}\right)^{-1}. \quad (1)$$

Given  $T_\alpha$ , we solve for  $\rho$  (Figure 2) using the triangle formed by the points  $e(0)$ ,  $p^*(N)$ , and  $e(N)$ . This yields

$$\rho = \pi - \sin^{-1} \left( (1 - T_\alpha^{-1}) \sin \alpha \right). \quad (2)$$

The specific steps of the simulation are given in Algorithm 2.1, and illustrated in Figure 3. The evader will calculate the pursuer's simulated location,  $\hat{p}$  as a function of the declared strategy  $\pi_p$  for  $N = T_\alpha \cdot d(0)$  steps. To construct an input measurement for each turn, the evader will first find  $b^*(t)$ , the orientation of the line  $\overline{\hat{p}(t)e(t)}$ , where  $e(t) = (d + t \cos \rho, t \sin \rho)$  for each turn  $t \in [1, N]$ . Then, the sequence  $B = \{b(1), \dots, b(N)\}$  is given by  $b^*(t) - \alpha$  for all  $N$  steps.

At the end of the simulation, the evader knows the pursuer's final location after  $N$  steps,  $\hat{p}(N)$  as a response to the measurement sequence  $B$ . The goal of the evader's strategy is to move to a final position  $e(N)$

---

**Algorithm 1** Evader Strategy:  $\pi_e(\alpha, d, \pi_p)$ 


---

```

 $T_\alpha \leftarrow \left(1 - \sqrt{\frac{1}{2 + 2 \cos \alpha}}\right)^{-1}$ 
 $\rho \leftarrow \pi - \sin^{-1} \left( (1 - T_\alpha^{-1}) \sin \alpha \right)$   $\triangleright$  Departure angle
 $\hat{p}(1) \leftarrow (0, 0)$   $\triangleright$  Simulated pursuer location
 $B \leftarrow \emptyset$   $\triangleright$  Generated bearing measurements
 $N \leftarrow T_\alpha \cdot d$   $\triangleright$  Optimal round length
for all  $t \in [1, N]$  do  $\triangleright$  Simulation Step
     $b^* \leftarrow$  orientation of the line connecting  $\hat{p}(t)$ 
and the point  $(d + t \cos \rho, t \sin \rho)$ 
     $B(t) \leftarrow b^* - \alpha$ 
     $\hat{p}(t + 1) \leftarrow \pi_p(\hat{P}, B)$ 
end for
if  $\hat{p}(N)$  on or below  $\overline{p\bar{e}}$  then  $\triangleright$  Evader response
    for all  $t \in [1, N]$  do
         $e(t) \leftarrow (d + t \cos \rho, t \sin \rho)$ 
        Give measurement  $B(t)$ 
    end for
else
    for all  $t \in [1, N]$  do
         $e(t) \leftarrow (d + t \cos \rho, -t \sin \rho)$ 
        Give measurement  $B(t)$ 
    end for
end if

```

---

which is on the opposite side of  $\overline{p\bar{e}}$  as the final pursuer position,  $\hat{p}(N)$ . We separate the result into two cases, and show in both cases the desired result is possible.

**Case 1** The final simulated pursuer position,  $\hat{p}(N)$ , is on or below the line  $\overline{p\bar{e}}$ .

In this case the evader will move along the path specified by  $e(t) = (d + t \cos \rho, t \sin \rho)$ , and generate bearing measurements  $B$ . Since the input does not change from the simulation,  $p(N)$  will be  $\hat{p}(N)$ , and the final position of the evader will be  $(d + N \cos \rho, N \sin \rho)$ .

**Case 2** The final simulated pursuer position,  $\hat{p}(N)$ , is above the line  $\overline{p\bar{e}}$ .

In this case, the evader will follow a different trajectory,  $E'$  which is the reflection of  $E$  about  $\overline{p\bar{e}}$ . Or,  $e(t)$  is the point  $(d + t \cos \rho, -t \sin \rho)$  for all  $t \in [1, N]$ . Assuming  $B$  does not change, the pursuer will again follow the simulated output,  $\hat{p}$ , and arrive at  $p(N)$  at the end of the round, this case is similar to the previous case: Both pursuer and evader are on the opposite side of  $\overline{p\bar{e}}$ . We now show the bearing measurements  $B$ , do not need to change while the evader is moving along the path  $E'$ . To proceed, we need the following structural lemma.

**Lemma 1** As shown in Figure 5, let  $\ell_1$  and  $\ell_2$  be two parallel lines separated by perpendicular distance  $d$ . Place any two non-coincident points on  $\ell_2$ ,  $p_1$  and

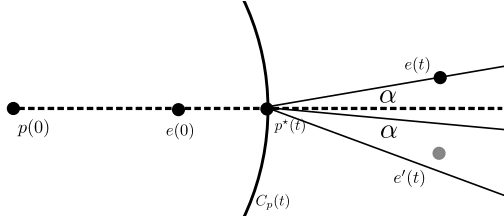


Figure 4: An illustration of Lemma 2: An evader at position  $e$  or  $e'$  can generate the measurement  $b(t)$  because the angle  $\widehat{ep^*e'}$  is less than  $2\alpha$ .

$p_2$ , separated by distance  $s > 0$ . Now consider a third point at distance  $d$  or greater from  $\ell_2$ ,  $x$ . The function  $\beta(x) = \widehat{p_1xp_2}$  is maximized at  $x^*$ , which is at distance  $d$  along the perpendicular bisector of  $p_1$  and  $p_2$ .

**Proof.** The function  $\beta(x)$  is the angle between the two points  $p_1$  and  $p_2$  from the point  $x$ , as shown. First, notice if  $x$  is anywhere left of the line,  $\ell_1$ , we can move the point toward the centroid of  $p_1$  and  $p_2$  and strictly increase the angle  $\beta(x)$ . Thus, the point maximizing  $\beta(x)$  is on the line  $\ell_1$ .

Without loss of generality, let  $p_1$  be at the point  $(d, \frac{s}{2})$  and  $p_2$  be at  $(d, -\frac{s}{2})$ , and let the coordinates of the point  $x$  be  $(0, y)$ .

$$\beta(x) = \tan^{-1}\left(\frac{\frac{s}{2} - y}{d}\right) + \tan^{-1}\left(\frac{\frac{s}{2} + y}{d}\right) \quad (3)$$

It can be verified the maximum of the function occurs when  $y = 0$ , corresponding to the point  $x$  being along the perpendicular bisector of  $p_1$  and  $p_2$ .  $\square$

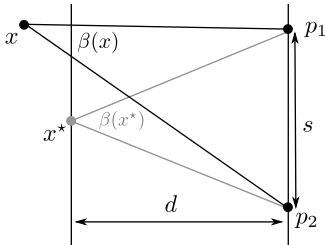


Figure 5: An illustration of Lemma 1: The angle  $\widehat{p_1xp_2}$ , labelled  $\beta(x)$ , is maximized at the distance  $d$  along the perpendicular bisector of  $p_1$  and  $p_2$ .

We are now ready to prove the evader can take either trajectory,  $E$  or  $E'$ , and still generate the same measurement sequence  $B$ .

**Lemma 2** Let  $E'$  be the sequence of evader positions given by  $\{(d + t \cos \rho, -t \sin \rho) : t = [1, N]\}$ , and  $E$  be the sequence of evader positions given by  $\{(d + t \cos \rho, t \sin \rho) : t = [1, N]\}$ . The bearing measurement sequence  $B$  described in Algorithm 2.1 can be generated by an evader following either  $E$  or  $E'$ .

**Proof.** As shown in Figure 4, the pursuer at every time step is inside the circle denoted  $C_p(t)$  of radius  $t$  centered on  $p(0)$ . Let  $\beta(t)$  be the angle  $\widehat{e(t)p(t)e'(t)}$ . By Lemma 1, the position  $p(t)$  which maximizes the angle  $\beta(t)$  is at the intersection of the  $x$  axis and the boundary of  $C_p(t)$ . We call this point  $p^*(t)$  and the corresponding angle  $\beta^*(t)$ .

Let the distance between  $p^*(t)$  and the line  $\overline{e(t)e'(t)}$  be  $d(t)$ . For all  $t \in [1, N]$  the following holds.

$$d(t) = d(0) + t(\cos \rho - 1) \quad (4)$$

Note the minimum value is at  $t = N$  and  $d(N) > 0$  by design. The separation between  $e(t)$  and  $e'(t)$  is,

$$s(t) = |e(t) - e'(t)| = 2t \sin \rho \quad (5)$$

which is maximized when  $t = N$ . The angle,  $\beta^*(t)$  satisfies the following.

$$\beta^*(t) = 2 \cdot \tan^{-1}\left(\frac{s(t)}{2d(t)}\right) \quad (6)$$

Recall  $\tan^{-1}(x)$  is monotone in  $x$  and the argument  $\frac{s(t)}{2d(t)}$  is maximized at  $t = N$ . Therefore  $\beta^*(t)$  is maximized when  $t = N$ . By inspecting Figure 2 we see,

$$\beta^*(t) = 2 \cdot \tan^{-1}\left(\frac{d(N) \sin \alpha}{d(N) \cos \alpha}\right) \quad (7)$$

which implies  $\beta^*(N) = 2\alpha$ , or  $\beta(t) \leq 2\alpha$  for all  $t \in [1, N]$ .

Consider the measurements  $B$  from the evader's simulation (Algorithm 2.1). Recall each  $b(t)$  was given by the angle to the point  $e(t)$  from  $p(t)$ , minus  $\alpha$ . We have just proven the angle  $\widehat{e(t)p(t)e'(t)}$  is less than  $2\alpha$  for any  $p(t)$ , as illustrated in Figure 4.

Thus, the angle between  $b(t)$  and  $e'(t)$  is less than  $\alpha$  for all  $p(t)$  and an evader at  $e'(t)$  can use an offset less than  $\alpha$  to generate the same measurement  $b(t)$  for all  $t \in [1, N]$ .  $\square$

The previous lemmas show that the evader can always end up in Case 1, either by directly following trajectory  $E$ , or by following an alternate trajectory  $E'$ , with the choice resolved by the simulation before the first move is made by either player. Thus, the ending configuration is as shown in Figure 2. We are now ready to prove the first main result of the paper: That each application of the evader's strategy yields a constant-factor increase in the distance between the pursuer and evader.

**Lemma 3** For any deterministic pursuer strategy,  $\pi_p$ , an evader distance  $d(0)$  away with maximum bearing offset  $\alpha$ , using Algorithm 2.1 produces a final separation after  $N$  turns satisfying  $d(N) = \eta \cdot d(0)$  with  $\eta > 1$  when  $\alpha > 0$ .

**Proof.** The proof follows directly from the configuration of the players at the end of the round. As shown in Figure 2,

$$[T_\alpha d(0)]^2 = [d(N) \sin \alpha]^2 + [(T_\alpha - 1)d(0) + d(N) \cos \alpha]^2 \quad (8)$$

After some manipulation, we solve for  $d(N)$  as a function of  $d(0)$  as follows.

$$d(N) = d(0) \left[ \sqrt{\cos^2 \alpha (T_\alpha - 1)^2 + 2T_\alpha - 1} - \cos \alpha (T_\alpha - 1) \right] \quad (9)$$

We call the term in brackets in the previous equation  $\eta$ , and note  $T_\alpha > 1$  by design making  $\eta > 1$  for any positive  $\alpha$ .  $\square$

We now consider *repeated* applications of the evader's strategy e.g., after playing for some large time,  $t$ . Since each round increases the separation between the players by a constant factor, and the length of the round is also proportional to the separation at the start of the round, we expect a logarithmic number of rounds played before any time  $t$ . We combine the logarithmic number of rounds played before a given time  $t$ , with the exponential increase to prove the following: the distance will increase at a rate proportional to the time  $t$ .

**Theorem 4** *For any deterministic pursuer strategy,  $\pi_p$ , an evader using repeated applications of the strategy given in Algorithm 2.1 increases the distance to the pursuer,  $d(t)$ , at a linear rate. At the end of  $t$  turns playing, the distance satisfies the following at the end of each evader round.*

$$d(t) \geq \gamma \cdot t + d(0) \quad (10)$$

$$\text{with } \gamma = \left( \sqrt{\frac{2}{1 + \cos \alpha}} - 1 \right) \quad (11)$$

**Proof.** Given the result of Lemma 3, we see the first round takes time  $T_\alpha d(0)$ , and produces  $d(1) = \beta d(0)$ . Continuing, the  $i^{\text{th}}$  round takes time  $T_\alpha \cdot d(i-1)$ , and produces end-of-round separation  $d(i) = \beta d(i-1)$ . Or, after expansion back to the first round,  $d(i) = \beta^i d(0)$ .

For any time  $t$ , which falls at the end of  $n$  rounds, the following holds.

$$t = \sum_{i=0}^n T_\alpha \cdot (\beta^i d(0)) \quad (12)$$

Which implies  $n = \log_\beta \left( 1 + t \frac{\beta-1}{T_\alpha \cdot d(0)} \right)$ . At the end of these  $n$  rounds, the separation is,

$$d(t) = d(0) \beta^n \quad (13)$$

$$= d(0) \beta^{\log_\beta \left( 1 + t \frac{\beta-1}{T_\alpha \cdot d(0)} \right)} \quad (14)$$

$$= d(0) + t \frac{\beta-1}{T_\alpha} \quad (15)$$

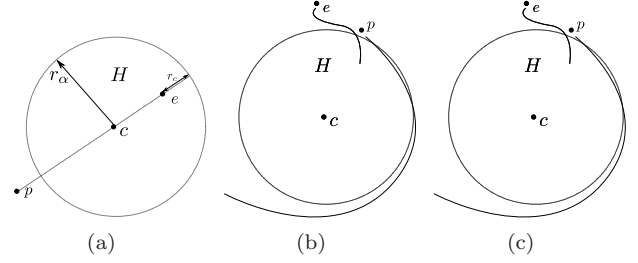


Figure 6: **a)** The lion-and-man starting configuration. At the start of the game, the evader chooses his location diametrically opposite the pursuer's location. **b)** The three-phase strategy starts when the pursuer enters (or starts within) the *home region*  $H$ , a circle of radius  $r_\alpha$ , or moves to within distance  $2r_c$  of the evader. The boundary of the arena is assumed to be much larger than  $r_\alpha$ , but is upper-bounded in Theorem 7. **c)** After sufficiently increasing the distance between players (Phase 1), and inducing an angular offset (Phase 2) the evader dashes back to the home region, re-entering without being captured (Phase 3).

Note the constant  $\beta$  contains both  $T_\alpha$  and  $\alpha$ . It can be verified the choice of  $T_\alpha$  given in Equation (1) maximizes  $\frac{\beta-1}{T_\alpha}$  when  $\alpha \in (0, \frac{\pi}{2}]$ , and produces a rate of increase as given in the theorem statement.  $\square$

### 3 The Lion and Man Game

We now investigate the effect of uncertain bearing measurements in the context of the classical Lion-and-Man game. The game is played in a circular arena. At the beginning of the game, the pursuer specifies a starting location  $p(0)$  followed by the evader choosing a starting location  $e(0)$ . The game proceeds in turns. First, the pursuer obtains a measurement, i.e. the angle to the evader,  $b(t)$ . As before, due to uncertainty,  $b(t) = b^*(t) + \alpha(t)$  where  $b^*$  is the orientation of the line through the two players, adjusted by  $\alpha(t)$ , an angle of the evader's choosing up to absolute value  $\alpha$ . The pursuer moves to a point contained inside the arena and within the step size which is normalized to one unit. We again assume the pursuer must choose a deterministic strategy  $\pi_p$  which is a function of the bearing measurements and his prior locations. After the pursuer's move, if the evader is within a fixed radius ( $r_c$ ) the pursuer wins the game. Otherwise, the evader may make his move of up to one unit distance in the same way as the pursuer.

To win the Lion-and-Man game, the evader (the man) must maintain a separation from the pursuer (the lion) which is greater than the capture radius ( $r_c$ ), regardless of the pursuer strategy. We will show it is possible: For any given  $\alpha > 0$ , there exist environments in which the evader can forever escape a deterministic pursuer.

The evader's strategy proceeds in three phases, each

illustrated in Figure 6. During the first phase, the evader will move away from the lion and repeatedly use Algorithm 1 to increase the separation between the players. In the second phase, the evader will execute a local maneuver, which ensures the man is offset from the line between the center of the arena and the pursuer by an angle greater than  $\frac{\alpha}{3}$ . In Phase 3, the evader will exploit the separation between itself and the lion to make a dash toward the center of the arena. When it is “close enough” to the center, the evader will start over from Phase 1. In the remainder of the paper we will show the evader can repeat these three steps indefinitely while avoiding capture, regardless of the lion’s strategy.

### 3.1 Evader’s Winning Strategy

We now present the strategy for the evader to win the Lion-and-Man game. The technical details of the three phases are given as separate proofs (Corollary 1 and Lemmas 5- 6). Following, we show the three phases, taken together, produce a repeatable evader strategy in Theorem 7.

The starting configuration is depicted in Figure 6(a). As shown, let  $c$  be the center of the arena. The evader will identify a *home region*  $H$  inside the arena where  $H$  is a circle centered at  $c$ . The radius of  $H$ ,  $r_\alpha$  is a function of  $\alpha$  and  $r_c$  and specified in Theorem 7. Let the pursuer start at location  $p$ , at distance  $r_p$  from  $c$ . The evader will choose to start inside the boundary of  $H$  at distance  $r_\alpha - 2r_c$  diametrically opposite the pursuer. Before the first Phase, the evader will simply wait until the pursuer enters  $H$ . Then, the evader will move directly away from the pursuer’s current location until he reaches the boundary of  $H$ . At this time, Phase 1 begins.

The beginning of Phase 1 is illustrated in Figure 6(a). In Phase 1, the evader will repeatedly apply the distance-increasing strategy from Section 2 (Algorithm 2.1). Each application of the strategy is called a round, and Phase 1 ends when enough rounds have been completed to increase the separation between the players to a desired distance  $d > \frac{1}{\sin \frac{\alpha}{3}}$ . The key to the analysis of Phase 1 is to show that the players do not travel an unbounded distance from the center of the arena. Since Theorem 4 provides a lower bound on the separation between the players as a function of the number of turns spent, we can bound the number of turns required in Phase 1 as follows.

**Corollary 1 (Effect of Phase 1)** *Let the distance between the pursuer and evader at the start of Phase 1 be  $d(0) \geq r_c$ . After  $T$  turns, the separation is greater than  $d(T) \geq \gamma T$ , where  $\gamma = \frac{1}{\cos \frac{\alpha}{2}} - 1$ , is given in Theorem 4. For any given desired separation  $d$ ,  $T \leq \frac{d}{\gamma} = d \left( \frac{\cos \frac{\alpha}{2}}{1 - \cos \frac{\alpha}{2}} \right)$  turns are required.*

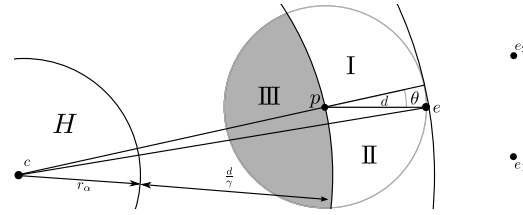


Figure 7: At the end of Phase 1 the pursuer  $p$  and evader  $e$  are separated by a distance  $d$  given in Corollary 1. At the start of Phase 2, the evader examines the angle  $\theta$ . If  $\theta > \frac{\alpha}{3}$  the evader can move on to Phase 3. Otherwise, he chooses his next move based on the next pursuer location, in region I, II, or III, as stated in Lemma 5

After Phase 1, the players are in the configuration shown in Figure 7. Let the pursuer’s distance from  $c$  at the end of Phase 1 be  $r_p$ , and let  $C_r$  be the circle of radius  $r_p$  centered on  $c$ . Similarly, let  $r_e$  be the distance of the evader from  $c$ . Because the players traveled at most distance  $\frac{d}{\gamma}$  from the region  $H$ , we know Phase 1 ensures  $r_p \leq r_\alpha + \frac{d}{\gamma}$ . Since the distance between the players is  $d$ , we know Phase 1 also ensures  $r_e \leq r_\alpha + d(1 + \frac{1}{\gamma})$ . The evader will check the angle  $\theta$ , which is the orientation of the line  $\overline{pe}$  with respect to the line  $\overline{cp}$  (i.e., the angle  $\pi - \widehat{epc}$ ), as labelled in Figure 7. If  $\theta > \frac{\alpha}{3}$ , the evader will move on to Phase 3. Otherwise, the evader must make a local move (Phase 2) to create the desired value of  $\theta$  as described next.

First, the evader will wait until the pursuer makes a move outside the circle  $C_p$  or  $\theta \geq \frac{\alpha}{3}$ . While the pursuer remains inside  $C_p$ , the evader does not need to take any action, and does not adjust the pursuer’s bearing measurements from their true value. When the pursuer exits the circle  $C_p$ , and  $\theta$  is still less than  $\frac{\alpha}{3}$ , the evader will begin a simulate step, exactly as described in Section 2, for  $d$  turns (just enough time for the pursuer to reach the evader’s initial location,  $e$ ).

Let  $e_1$  and  $e_2$  be two points, offset by  $\pm\alpha$  from the line  $\overline{pe}$  at distance  $d$  from  $e$ . As before, the evader constructs the bearing measurement sequence to be the orientation between the current simulated pursuer location  $\hat{p}(i)$  and the point distance  $i$  along the line segment  $\overline{ee_2}$ , starting at the point  $e$  when  $i = 0$ . As before the bearings are offset by negative  $\alpha$ .

Let  $\hat{p}$  be the final pursuer location after the simulated move. First, if  $\hat{p}$  is inside the circle  $C_p$  (in region III in Figure 7), the evader does not need to take any action, and will continue to wait in Phase 2. Otherwise, we partition the possible locations of  $\hat{p}$  into two sets, I and II, divided by the line  $\overline{ce}$ , as shown in Figure 8(a) and 8(b), respectively. If  $\hat{p} \in I$ , the evader will choose to move to  $e_1$ , otherwise he moves to  $e_2$ . In such a case, Phase 2 ends when the evader reaches  $e_1$  or  $e_2$  after  $d$  turns.

We use the following lemma to show the configuration of the players after Phase 2.

**Lemma 5 (Effect of Phase 2)** *Let  $p$  and  $e$  be the pursuer and evader position after Phase 1 as shown in Figure 8. Consider the point  $\hat{p}$ , at most distance  $d$  from  $p$ , and falling into region I or II (outside the radius  $r_p$ ). For any such  $\hat{p}$  there exists a corresponding point  $\hat{e}$ , at most distance  $d$  from  $e$  such that all of the following hold.*

1. *Max  $r_p$ : The distance between  $\hat{p}$  and  $c$  is at most  $d(1 + \frac{1}{\gamma}) + r_\alpha$*
2. *Max  $r_e$ : The distance between  $\hat{e}$  and  $c$  is at most  $r_p + d = d(2 + \frac{1}{\gamma}) + r_\alpha$*
3. *Separation: The distance between  $\hat{p}$  and  $\hat{e}$  is at least  $d$ .*
4. *Angular Offset: The angle  $\theta$ , which is measured between the line  $\overline{\hat{p}\hat{e}}$  and the line  $\overline{c\hat{p}}$  is at least  $\frac{\alpha}{3}$ .*

**Proof.** As illustrated in Figure 8, Let  $c$  be the center of the playing environment. Let the pursuer be at position  $p$  and radius  $r_p$  from  $c$ , and the evader be at radius  $r_e \geq r_p + d$ . From Corollary 1, we know the players travelled at most distance  $\frac{d}{\gamma}$  after exiting  $H$  and the evader is distance  $d$  away.

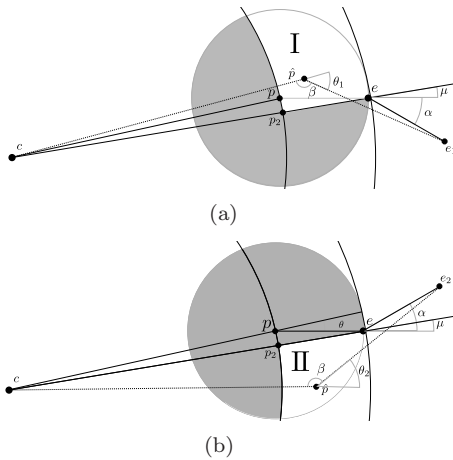


Figure 8: **a and b)** By Lemma 5, the evader can choose to move to location  $e_1$  or  $e_2$ , based on the pursuer's chosen location in region I or II, producing  $\theta_1$  or  $\theta_2$  greater than  $\frac{\alpha}{3}$ , respectively. If the pursuer moves to region III, the evader will remain at position  $e$ .

For any pursuer location,  $\hat{p}$ , and evader location  $\hat{e}$ , we notice the first two conditions stated in the theorem hold, since the evader and pursuer move at most distance  $d$ . Also note for any  $\hat{p}$  above (resp. below) the line  $\overline{ce}$ , the point  $e_1$  (resp.  $e_2$ ) is at least distance  $d$  away, since  $l(\overline{ce_1}) = d$  and  $l(\overline{ce_2}) = d$ . It remains to show the evader has achieved an angular offset as stated.

Consider case I:  $\hat{p} \in I$ , and the evader has moved to  $e_1$ , as illustrated in Figure 8(a). Let  $\beta$  be the angle  $\widehat{e_1\hat{p}c}$ , implying  $\theta_1 = \pi - \beta$ . Of all  $\hat{p} \in I$ ,  $\beta$  is maximized ( $\theta_1$  minimized) when  $\hat{p} = p_2$ . To see this, draw the line  $\overline{ce_1}$ , find its midpoint, and recall from Lemma 1  $\beta$  increases by moving  $\hat{p}$  toward the midpoint. We now show  $\theta_1 \geq \frac{\alpha}{3}$ .

First find the perpendicular projection of  $e_1$  onto the line  $\overline{ce}$ . The distance of the projection from the point  $p_2$  is  $d + d \cos(\alpha + \mu)$ . The length of the projection is  $d \sin(\alpha + \mu)$ . Since  $\tan \theta_1 = \frac{d \sin(\alpha + \mu)}{d + d \cos(\alpha + \mu)} = \tan(\frac{\alpha + \mu}{2})$ ,  $\theta_1 > \frac{\alpha}{2}$ .

Consider case II:  $\hat{p} \in II$ , and the evader has moved to  $e_2$ , as illustrated in Figure 8(b). By a similar argument as before, we see  $\beta$  is maximized when  $\hat{p} = p_2$ . We again find the projection of  $e_2$  onto the line  $\overline{ce}$ , which has length  $d \cos(\alpha - \mu)$ , and intersects  $\overline{ce}$  at distance  $d + d \sin(\alpha - \mu)$  from  $p_2$ . Now, we note  $\mu < \theta < \frac{\alpha}{3}$  by assumption. Therefore  $\tan \theta_2 > \frac{d \sin(\frac{2\alpha}{3})}{d + d \cos(\frac{2\alpha}{3})}$  which implies  $\theta_2 > \frac{\alpha}{3}$ . Thus, all four conditions are proved.  $\square$

To recap the result of Phase 1 and 2, we know the pursuer is inside a circle  $C_p$ , with radius  $r_p \leq r_\alpha + d(1 + \frac{1}{\gamma})$ , and the evader is inside the circle  $C_e$  with radius  $r_e \leq r_p + d$ . We also know the evader is offset from the line  $\overline{cp}$  by an angle at least  $\frac{\alpha}{3}$  and is distance at least  $d$  from the pursuer. The evader will now move on to the last phase. Now the evader will move at an angle from the line  $\overline{pe}$ , given by  $\frac{\pi}{2} + \phi$ , where  $\phi = \theta - \sin^{-1} \frac{r_c}{d}$ . The angle  $\phi$  is chosen so for any  $r_c$ , there exists a separation  $d$  which makes it possible for the evader to move closer to the center of the arena without being captured. This move is called Phase 3, and is illustrated in Figures 9(a) and 9(b).

**Lemma 6 (Effect of Phase 3)** *Let  $c$  be the center of the playing circle, and a pursuer with capture radius  $r_c$  be distance  $r_p$  from the  $c$ . Let the evader be distance  $d$  away from the pursuer, and offset from the line between the pursuer and center of the circle by an angle  $\theta$ . The evader can reach a point distance  $r^*$  from the center of the circle without being captured where  $r^*$  satisfies*

$$r^* \leq r_p \cos(\phi) + \sqrt{d^2 - r_c^2} \quad (16)$$

$$\text{with } \phi = \theta - \sin^{-1} \left( \frac{r_c}{d} \right) > 0. \quad (17)$$

**Proof.** For simplicity, let us consider the case of  $r_c = 0$  as illustrated in Figure 9(a). The locus of all points equidistant from  $p$  and  $e$  is given by the perpendicular bisector of the line  $\overline{pe}$ , which we label  $\ell$ . By travelling parallel to  $\ell$  the evader can reach the point  $e_2$  before the pursuer can. Since the line  $\overline{pe}$  and  $\overline{ce_2}$  are parallel, we see the angle  $\widehat{pce_2}$  is exactly  $\theta$ . The distance  $l(\overline{pe_2})$  is given by  $r_p \cos \theta + l(\overline{pe}) = r_p \cos \theta + d$ , as desired.

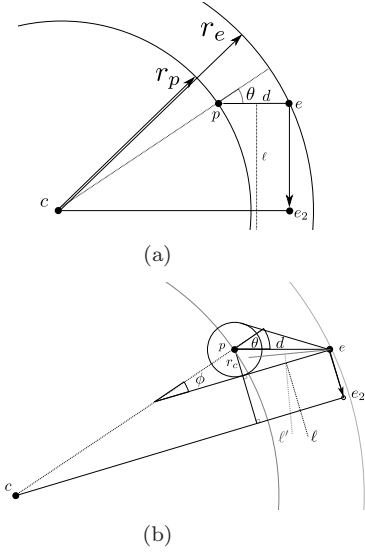


Figure 9: During Phase 2, the evader will move at an angle  $\phi + \frac{\pi}{2}$ , where  $\phi$  is measured with respect to the line from the center of the circle to the point  $p$ . After Phase 2, the evader is at position  $e_2$ . Lemma 5 shows  $\theta \geq \frac{\alpha}{3}$  and bounds  $r_p$  and Lemma 6 bounds the distance from the center to  $e'$ . Note  $\phi = \theta - \sin^{-1} \frac{r_c}{d}$  and  $d$  is chosen such to ensure  $\phi > 0$ .

In the case of  $r_c > 0$ , the evader modifies his strategy as follows. We observe escaping capture by a pursuer with  $r_c > 0$  is the same as escaping any pursuer  $p'$  with  $r_c = 0$ , when the initial position of  $p'$  is at most distance  $r_c$  from the point  $p$ . We will find an escape path for the evader along which no  $p'$  which can achieve capture.

To proceed we draw a line tangent to the circle of radius  $r_c$  and passing through  $e$ . Let the tangent point on the circle be  $p_t$ . The evader will travel parallel to the perpendicular bisector of the line segment  $\overline{ep_t}$ , labelled  $\ell$  until he reaches the location closest to  $c$ , labelled  $e_2$  in Figure 9(b).

To see the evader can reach  $e_2$  without being captured, consider any pursuer with no capture radius ( $r_c = 0$ ) at location  $p'$ , at most distance  $r_c$  from the point  $p$ . Let  $\ell'$  be the perpendicular bisector of the line  $\overline{ep'}$ . For any  $p' \neq p_t$ , the line  $\ell'$  rotates away from  $e_2$ , leaving  $e_2$  safely on the evader's side. For any  $p'$  closer to  $e$ , the line  $\ell'$  moves closer to  $e_2$ , but for  $e_2$  to lie on  $\ell'$ ,  $p'$  must be coincident with  $e$ . Since the evader enters Phase 2 with separation  $d > 0$ , this is not possible.

To find the inner radius, note  $\overline{ce_2}$  is parallel with the line passing through  $e$  and tangent to the capture circle, implying  $\widehat{pce_2}$  is exactly  $\theta - \sin^{-1}(\frac{r_c}{d})$ . The distance  $l(\overline{pe_2})$  is given as stated in the lemma.  $\square$

We now show the evader ends in the home region,  $H$ . After entering the home region, the evader can

continue to move directly away from the pursuer's location. Upon exiting  $H$ , the game has reset, and the evader can start over in Phase 1, repeating indefinitely.

**Theorem 7** Let  $\phi$  be  $\frac{\alpha}{3} - \sin^{-1} \frac{r_c}{d}$ , and let  $d$  be any constant greater than  $\frac{r_c}{\sin \frac{\alpha}{3}}$ . Let  $\gamma$  be the constant  $\left(\sqrt{\frac{2}{1+\cos \alpha}} - 1\right)$  from Theorem 4. An evader beginning inside a circle  $H$  of radius  $r_\alpha = \frac{d(1+\frac{1}{\gamma})\cos \phi + \sqrt{d^2 - r_c^2}}{1 - \cos \phi}$  can, after all three phases described, return to the circle  $H$  without being captured.

**Proof.** By assumption, the radius of  $H$  is  $r_\alpha = \frac{d(1+\frac{1}{\gamma})\cos \phi + \sqrt{d^2 - r_c^2}}{1 - \cos \phi}$ . After Phase 2, as stated in Lemma 5, the pursuer is at most distance  $r_p = r_\alpha + d(1 + \frac{1}{\gamma})$  from the center,  $c$ .

$$r_p = \frac{d(1 + \frac{1}{\gamma})\cos \phi + \sqrt{d^2 - r_c^2}}{1 - \cos \phi} + d(1 + \frac{1}{\gamma}) \quad (18)$$

We now apply Lemma 6 to find the inner radius reachable by the evader. Let the inner radius be  $r^*$ .

$$r^* = \left[ \frac{d(1 + \frac{1}{\gamma})\cos \phi + \sqrt{d^2 - r_c^2}}{1 - \cos \phi} + d(1 + \frac{1}{\gamma}) \right] \cos \phi + \sqrt{d^2 - r_c^2} \quad (19)$$

After distributing  $\cos \phi$  and the denominator we have,

$$r^* = \frac{d(1 + \frac{1}{\gamma})\cos^2 \phi + \sqrt{d^2 - r_c^2}\cos \phi}{1 - \cos \phi} + \frac{d(1 + \frac{1}{\gamma})\cos \phi(1 - \cos \phi) + \sqrt{d^2 - r_c^2}(1 - \cos \phi)}{1 - \cos \phi} \quad (20)$$

$$= \frac{d(1 + \frac{1}{\gamma})\cos \phi(\cos \phi + 1 - \cos \phi)}{1 - \cos \phi} + \frac{\sqrt{d^2 - r_c^2}(\cos \phi + 1 - \cos \phi)}{1 - \cos \phi} \quad (21)$$

$$= \frac{d(1 + \frac{1}{\gamma})\cos \phi + \sqrt{d^2 - r_c^2}}{1 - \cos \phi} \quad (22)$$

Thus, at the end of Phase 3, assuming  $r_\alpha$ ,  $\phi$ , and  $d$  are chosen as stated, the evader is again inside the home region,  $H$  and is outside the capture radius of the pursuer.  $\square$

#### 4 Concluding Remarks

In this paper, we studied novel pursuit-evasion games in which the pursuer can obtain only uncertain bearing



measurements. We showed that the evader can exploit bearing uncertainty to change the outcome of the game in his favor in two classical games.

In the games we considered, there is only one pursuer and the players have the same maximum speed. It is likely that the evader can be captured by either increasing the number of pursuers or the maximum speed of the (single) pursuer. Obtaining bounds for these versions are interesting avenues for future research.

Another avenue is to allow randomization in pursuer strategies. The evader strategy in the open plane can be modified to work against randomized strategies since this game is infinite. In the lion-and-man game however, when the pursuer can measure the true location, the number of steps until capture is finite. It is plausible that by discretizing the disk, we can obtain a finite set containing all pursuit strategies. No matter which strategy the evader plays, at least one element of this set would capture the evader and this strategy can be “guessed” using randomization. Hence the evader can be captured even without any measurements. The capture time resulting from this argument would be exponential in the duration of the game. In [7], it was shown that the capture time is indeed exponential when the game takes place on arbitrary graphs. Whether this bound can be improved when bearing measurements are available is left for future research.

### Acknowledgement

This work was supported by the National Science Foundation (#1111638, #0917676, and #1317788). Josh gratefully acknowledges ongoing support from the MN ARCS Foundation.

### References

- [1] J. E. Littlewood, *Littlewood’s miscellany*. Cambridge University Press, 1986.
- [2] T. H. Chung, G. A. Hollinger, and V. Isler, “Search and pursuit-evasion in mobile robotics: A survey,” *Autonomous robots*, vol. 31, no. 4, pp. 299–316, 2011.
- [3] P. Tokekar, E. Branson, J. Vander Hook, and V. Isler, “Tracking aquatic invaders,” *IEEE Robotics and Automation Magazine*, vol. 20, no. 3, pp. 447–452, September 2013.
- [4] L. Alonso, A. S. Goldstein, and E. M. Reingold, “Lion and man: upper and lower bounds,” *ORSA Journal on Computing*, vol. 4, no. 4, pp. 447–452, 1992.
- [5] G. Rote, “Pursuit-evasion with imprecise target location,” in *Proceedings of the Fourteenth Annual ACM-SIAM Symposium on Discrete Algorithms (SODA)*. Society for Industrial and Applied Mathematics, 2003, pp. 747–753.
- [6] K. Klein and S. Suri, “Trackability with Imprecise Localization,” *arXiv preprint arXiv:1312.6573*, 2013. [Online]. Available: <http://arxiv.org/abs/1312.6573>
- [7] V. Isler and N. Karnad, “The role of information in the cop-robber game,” *Theoretical Computer Science*, vol. 399, no. 3, pp. 179–190, 2008.

### A Notation and Constants

- $p$  The pursuer’s current position.  $p(t)$  is used for time-indexed positions.
- $e$  The evaders’s current position.  $e(t)$  is used for time-indexed positions.
- $b^*(t)$  the orientation of the line  $\ell$  in a fixed world coordinate frame at the start of turn  $t$ .
- $\widehat{abc}$  the angle formed by the points  $a$ ,  $b$ , and  $c$
- $\overline{ab}$  the line passing through points  $a$  and  $b$
- $l(\overline{ab})$  the length of the line segment connecting points  $a$  and  $b$
- $b(t)$  The pursuer’s measurement of the orientation of  $\overline{pe}$ , as adjusted by the evader during turn  $t$ .
- $\alpha$  The evader’s maximum angular disturbance of  $b(t)$
- $C(a, r)$  a circle centered on point  $a$  of radius  $r$
- $r_c$  The capture radius of the pursuer, as used in the Lion-and-Man game.
- $T_\alpha$  The optimal duration of Algorithm 1 is given by  $T_\alpha \cdot d$ , where  $d$  is the distance between the players at the start of the algorithm. Defined in Equation 1
- $\gamma \left( \sqrt{\frac{2}{1+\cos \alpha}} - 1 \right)$  The rate at which an evader can increase the distance between himself and a pursuer, defined in Equation 11.
- $\alpha$  The maximum angular disturbance in the pursuer’s bearing measurement.
- $\rho$  The evader’s escape angle during the Open Plane Pursuit game. Defined in Equation 2 to be  $\pi - \sin^{-1}((1 - T_\alpha^{-1}) \sin \alpha)$
- $\theta$  The angle between  $\overline{cp}$  and  $\overline{pe}$ , or  $\widehat{cpe}$ .
- $\phi$  The evader’s escape angle during Phase 3 of the Lion and Man game. Defined in Theorem 7